Analytical Description of Metal Loss in Finite-Difference Transmission-Line Analysis

Marco Kunze, *Student Member, IEEE*, and Wolfgang Heinrich, *Senior Member, IEEE*

***Abstract*—A new approximate approach to include metallic loss of planar transmission lines in the finite-difference frequency-domain analysis is presented. From the two-dimensional field behavior in the vicinity and inside of nonideal metallic layers, analytical approximations are obtained and incorporated into the algorithm. This approach leads to considerable savings in computational efforts. The same mesh size as in the lossless case can be used at an acceptable accuracy level and skin depth does not need to be resolved. Furthermore, preprocessing can be automated. The benefits of the new method are demonstrated for typical monolithic microwave integrated circuit coplanar waveguides.**

***Index Terms*—Conductor loss, coplanar waveguides, finite-difference methods, MMICs, singular field behavior, skin effect, transmission-line analysis.**

I. Introduction

THE incorporation of *a priori* knowledge into transmission-line analysis is well known in computational electromagnetics. A typical example is the singular field behavior at microstrip discontinuities in conjunction with the spectral-domain approach (SDA) [1] or the finite-difference (FD) method [2]–[5]. The objective is to reduce numerical efforts while maintaining accuracy. This is the more important when miniaturized structures such as monolithic microwave integrated circuit (MMIC) coplanar lines are treated [6], [8], where conductor loss plays a significant role and skin depth needs to be resolved. Recently, the hybrid FD approach of [4] was extended to consider metal loss [6], [7], which allows discretization steps much larger than skin depth in the dynamic analysis (in the following, "dynamic" will be used for an analysis considering the full set of Maxwell's equations, whereas "quasi-static" refers to a simplified description where displacement currents are neglected and only conducting currents are included). The disadvantage of the hybrid method, however, is the preprocessing efforts: one needs to perform two separate runs; first, a quasi-static FD analysis with high resolution, and then, a dynamic FD analysis [6]. This procedure leads to dramatic savings in computational costs, but requires both additional computer resources and an experienced user.

The approach presented here—which we will refer to as the analytical hybrid FD method in the following—avoids this limitation. It relies on analytical expressions for the *a priori* knowledge and, thus, can be automated. For this purpose, closed-form approximations are developed for the electromagnetic field within rectangular planar conductors of finite conductivity ($\sigma < \infty$) and, in particular, in the vicinity of 90° conductor edges. These expressions are deduced under appropriate simplifying assumptions. In order to incorporate the known field behavior into the FD algorithm, the coefficients of the FD equations are locally multiplied with correction factors (see [7]). To demonstrate validity and benefits of this approach, it is applied to typical MMIC coplanar waveguides (CPWs) for both the even and the odd modes and compared to the conventional finite-difference frequency-domain (FDFD) formulation, as well as to mode-matching results [8].

The new formulation differs principally from previous impedance boundary or conducting sheet approximations (e.g., [13]) because finite thickness is retained in the analysis and two-dimensional (2-D) effects at the edges are accounted for.

Manuscript received November 8, 2000. This work was supported by the Deutsche Forschungsgemeinschaft under Contract He 1676/12.

The authors are with the Ferdinand-Braun-Institut für Höchstfrequenztechnik, D-12489 Berlin, Germany (e-mail: marcokunze@ieee.org).

Publisher Item Identifier S 0018-9480(02)04063-2.

II. Method

Our FD description starts from Maxwell's equations in integral form [see (1) and (2)] and applies a discretization on Yee's mesh according to the well-known finite-integration scheme [9]. A Cartesian coordinate system is used with z being the direction of wave propagation

$$\oint_{C(A)} \frac{\vec{B}}{\mu} \cdot d\vec{s} = \iint_{A} (j\omega\varepsilon\vec{E} + \sigma\vec{E}) \cdot d\vec{A} \tag{1}$$

$$\oint_{C(A)} \vec{E} \cdot d\vec{s} = -j\omega \iint_{A} \vec{B} \cdot d\vec{A}. \tag{2}$$

In order to take into account strong local changes of the electromagnetic field within nonideal metallic conductors and in the vicinity of edges, the conventional FD line and surface integral representations are multiplied by suitable correction factors, as shown in (3) and (4), respectively. F' denotes the discretized value of the E or B fields, respectively, Δl denotes a line segment of the integration path, and ΔA denotes the area of the corresponding cell face. cl and cf are the correction factors with $cleu(u = x, y)$ and $cfez$ referring to the electric and $cfmu$ to the magnetic fields, respectively,

$$\int_{l} F \cdot dl \approx F' \cdot \Delta l \cdot cl \tag{3}$$

$$\iint_{A} F \cdot dA \approx F' \cdot \Delta A \cdot cf. \tag{4}$$

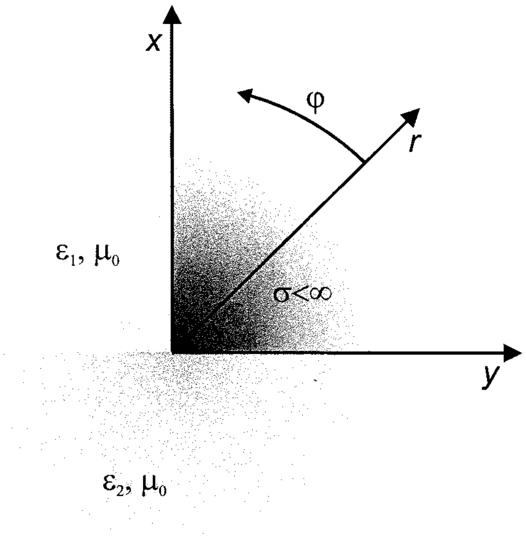

Fig. 1. Typical metallic edge geometry.

In the case of a longitudinally homogeneous transmission line, some integrals do not require correction because they neither involve singularities, nor strong local changes, thus, the conventional FD formulation suffices. For other quantities, the quantitative influence is small such that it does not make sense to introduce any refinement there. The latter is true, for example, for the transverse electric field *within* a conductor (also in the nonideal case) and the magnetic-field components normal to a conductor surface. The magnetic-field component B_z, on the other hand, is not affected due to longitudinal homogeneity. Briefly speaking, one finds that only the line integrals of the transverse electric-field component E_x, E_y at edges and the surface integrals of E_z, B_x, and B_y within conductors need correction.

The novel idea presented in this paper is to use analytical approximations to determine the correction factors for the fields within nonideal conductors of conductivity σ. Let us consider the case of such a rectangular conductor with an edge embedded in two different dielectrics, as shown in Fig. 1. The dielectric materials are characterized by real permittivities ε_1, ε_2, and the magnetic permeability μ_0. As derived in [10], the transverse electric-field components (E_x and E_y) tend to infinity according to an $r^{\nu-1}$ rule as distance r from the edge approaches zero, for both infinite and finite conductivity $\sigma < \infty$. In contrast to the case of ideal conductors, however, the transverse magnetic field (B_x and B_y) is bounded for $\sigma < \infty$. Nevertheless, the transverse magnetic and longitudinal electric field (E_z) inside the conductor is dominated by the skin effect and, therefore, may exhibit peaks with strong local changes near edges and the conductor surface, as illustrated in Fig. 2. This field behavior varies with frequency. In the dc limit, one has a homogeneous current distribution and, hence, at low frequencies, a smooth characteristic is found. In the high-frequency limit, where skin depth is smaller than the conductor dimensions, the fields in the conductor decay away from the surface and strong field gradients are observed. In the one-dimensional (1-D) case, this can be described easily by means of the well-known skin-effect law. In reality, however, 2-D effects show a significant influence. This is true particularly at the conductor edges. Therefore, a closed-form approximation of the 2-D field distribution will be derived in the following, which can be used to calculate the respective correction factors analytically.

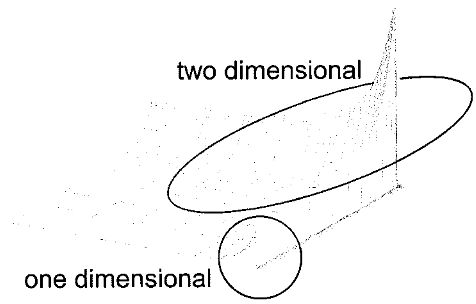

Fig. 2. Normalized plot of longitudinal current density $J_z = \sigma \cdot E_z$ at a conductor edge (frequency: 50 GHz, conductivity $\sigma = 3 \cdot 10^7$ S/m). The marked regions indicate whether the field behavior is approximately 1-D or 2-D.

We will start with the transverse electric field (E_x, E_y). These components are negligible *within* the conductors and, therefore, do not need a correction there, but only outside at the conductor edges, as in the case of infinite conductivity. The corresponding expression for $cleu$ is derived following [11] and [12] and given in (5), where ω denotes the angular frequency and ε_0 denotes the permittivity. Strictly speaking, as a consequence of finite conductivity, ν assumes a complex value, but its imaginary part is small and, for metallic conductivities, the real part has almost the same value as for the electrostatic solution with ideal conductors (for details, see [10])

$$cleu = \frac{1}{\nu \cdot 2^{1-\nu}}$$

where $\nu = (1/\pi) \cdot \arccos(-1 + Y)$ and

$$Y = \frac{\varepsilon_2 \cdot \left(-\varepsilon_1 - j \cdot \dfrac{\sigma}{\omega \cdot \varepsilon_0}\right)^2}{(\varepsilon_1 + \varepsilon_2) \cdot \left(\varepsilon_1 - j \cdot \dfrac{\sigma}{\omega \cdot \varepsilon_0}\right) \cdot \left(\varepsilon_2 - j \cdot \dfrac{\sigma}{\omega \cdot \varepsilon_0}\right)}. \tag{5}$$

For the transverse magnetic-field components B_x and B_y, one has a different situation. Inside the conductors, they show a skin-depth-related behavior. In this region, one finds that B_x and B_y can be approximated by a 1-D characteristic without significant loss of accuracy. Thus, we assume that the x- and y-components of the magnetic field $B_\nu(u)$ ($\nu = y, x, u = x, y$) follow the well-known skin-effect rule. This leads to (6) with Δu being the length of a Yee cell in the x- or y-directions and B'_ν denoting the discretized field value related to this cell

$$cfmu = \frac{\int_{-\Delta u/2}^{\Delta u/2} B_v(u)\, du}{B'_v \cdot \Delta u} = \frac{\sin\left(k \cdot \dfrac{\Delta u}{2}\right)}{k \cdot \dfrac{\Delta u}{2}}$$

where

$$B_v(u) = C \cdot e^{-j \cdot k \cdot u} + D \cdot e^{j \cdot k \cdot (u - \Delta u/2)}$$

and

$$k = (1 - j) \cdot \sqrt{\frac{\mu_0 \sigma \omega}{2}}. \tag{6}$$

The most complicated case is that of the longitudinal electric-field component E_z inside the conductor or, in other words, the current density $J_z = \sigma \cdot E_z$. As illustrated by Fig. 2, this field component exhibits an inherently 2-D behavior near conductor edges, whereas it approaches the classical 1-D case elsewhere. Since there is no analytical model available for the 2-D geometry, we choose an empirical approximation to describe the spatial dependence of E_z. It is based on high-resolution quasi-static FD calculations of the typical edge geometries for the frequency and conductivity range of interest. Equation (7) presents the formula for $E_z(x, y)$. It contains the classical skin-effect terms for x and y together with an additional expression accounting for the edge characteristic, which is related to the radius $r = (x^2+y^2)^{1/2}$. The constants K, b, and c are fitting factors, which were extracted from high-resolution FD calculations and found to be $K = 0.39$, $b = 0.664 + j \cdot 0.056$, and $c = 0.483 + j \cdot 0.006$. Note that all considerations refer to a coordinate system with its origin located at the edge (see Fig. 1). Accordingly, x and y basically denote the distances from the edge

$$E_z(x, y) = A \cdot \exp\left(-j \cdot k \cdot b \cdot \left(1 - c \cdot \arctan^2\left(\frac{y-x}{y+x}\right)\right) \cdot r\right) + K\left(e^{-j \cdot k \cdot x} + e^{-j \cdot k \cdot y}\right), \qquad \text{with } A = 1 - 2 \cdot K. \tag{7}$$

Equation (7) refers to a single edge. Usually, however, one has several edges in close vicinity, e.g., for thin planar conductors (see the coplanar geometry in Fig. 3). In this case, two edges occur, separated by the conductor thickness t. Both edges may then influence the E_z distribution and, correspondingly, the total electric field E_z inside the conductor has to be described by superposing the two contributions $E_z(x, y)$ and $E_z(t-x, y)$ according to (7) as follows:

$$E_{z\text{tot}}(x, y, t) = E_z(x, y) + E_z(t-x, y). \tag{8}$$

Equation (8) is then used to compute $cfez$ as given in (9). The formula refers to the node (x_0, y_0) of the Yee mesh, i.e., it provides the $cfez$ value for $E_{z\text{tot}}(x_0, y_0)$. This node has four neighboring cells, two in the x-direction and two in the y-direction. The variables Δu_i ($u = x, y$, $i = 1, 2$) represent the corresponding lengths of these cells. $\sigma(x, y)$ describes the conductivity as a function of x and y. It is constant inside the conductor and zero outside. Accordingly, $\sigma(x_0, y_0)$ denotes the conductivity and $E_z(x_0, y_0)$ denotes the discretized field value associated with the node (x_0, y_0)

$$cfez = \frac{\int_{x_0-\Delta x_1/2}^{x_0+\Delta x_2/2} \int_{y_0-\Delta y_1/2}^{y_0+\Delta y_2/2} \sigma(x, y) \cdot E_{z\text{tot}}(x, y, t)\, dx\, dy}{\sigma(x_0, y_0) \cdot E_{z\text{tot}}(x_0, y_0) \cdot \frac{\Delta x_2 + \Delta x_1}{2} \cdot \frac{\Delta y_2 + \Delta y_1}{2}} \tag{9}$$

with $E_z(x, y, t)$ according to (8).

Since we did not find a way to integrate the first term in (7) analytically, the integral in (9) is calculated numerically (Gauss–Legendre quadrature), which, is not a difficult task.

Using (8) ensures that $cfez$ can be computed accurately enough for rectangular conductors of arbitrary thickness $t > 0$.

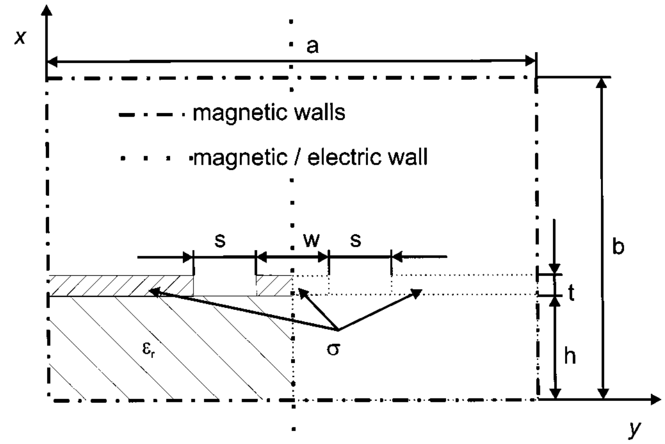

Fig. 3. Coplanar cross section under investigation (dimensions are $s = 20$ μm, $w = 10$ μm, $t = 3$ μm, $h = 500$ μm, $a = 450$ μm, $b = 1503$ μm, $\varepsilon_r = 12.9$, and conductivity $\sigma = 3 \cdot 10^7$ S/m. The center wall can be magnetic or electric depending on symmetry).

For thin conductors with $t \ll \delta$, where δ denotes skin depth, (8) approaches a constant value along the thickness direction. For thick conductors with $t \gg \delta$, on the other hand, the electric field E_z on both surfaces of a rectangular conductor behaves like that of a single edge. In the intermediate range, the influence of both edges has to be accounted for as realized by the superposition in (8). This is also the most critical range with regard to accuracy.

Regarding the remaining parameters, (7) and (8) hold for arbitrary frequencies f and conductivity values σ as long as frequency does not exceed the limit of quasi-TEM propagation. This is because (7), as well as the entire hybrid concept, are based on quasi-static arguments.

III. Results

In order to verify the analytical hybrid FD method, typical MMIC CPWs are studied, including even and odd modes, i.e., the coplanar mode and the slot-line type as well, which usually represents a parasitic mode. Fig. 3 shows the geometry. Due to symmetry, only one-half of the structure is considered introducing a magnetic and an electric wall at $x = a/2$ for the coplanar and slot-line modes, respectively. For the analytical hybrid FD method, a graded mesh, as in the lossless case (1350 cells), is used with its smallest cell size being approximately 1 μm. In contrast, the conventional FD analysis requires resolution of the skin depth δ, which leads to a much denser mesh (4248 cells), the smallest cell size of which being about ten times smaller ($\delta/3 = 0.1$ μm).

In Figs. 4–7, results of the analytical hybrid FD method are compared to the conventional FD formulation and mode-matching data [8]. Effective dielectric permittivity $\varepsilon_{r,\text{eff}}$, attenuation α, and the complex characteristic impedance Z_c are considered, treating a typical MMIC coplanar line with a fixed ground-to-ground spacing of 50 μm in the frequency range up to 100 GHz. Figs. 4 and 5 provide the results on effective permittivity $\varepsilon_{r,\text{eff}} = (\beta/\beta_0)^2$, attenuation α, and complex characteristic impedance Z_c. The ripple in the impedance Z_c around 55 GHz is caused by the first higher order substrate mode.

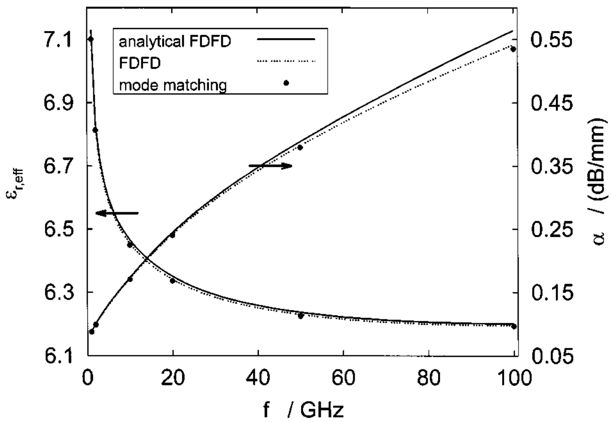

Fig. 4. CPW-mode effective permittivity $\varepsilon_{r,\,\mathrm{eff}}$ and attenuation α against frequency (data as in Fig. 3 with magnetic wall in the center); comparison of the new hybrid method (analytical FDFD) with the conventional FDFD method and mode-matching data [8].

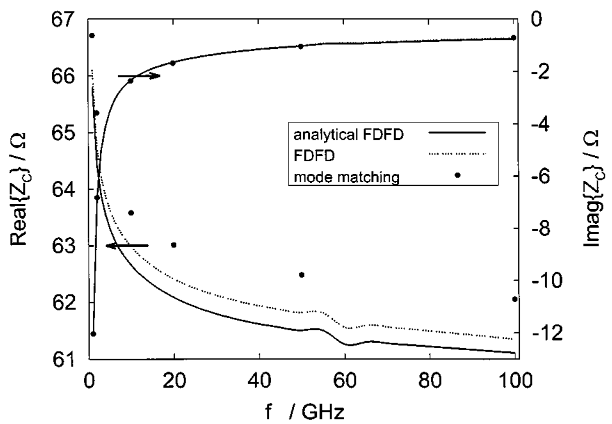

Fig. 5. CPW-mode complex characteristic impedance Z_c (voltage–current definition) against frequency (other data as in Fig. 4).

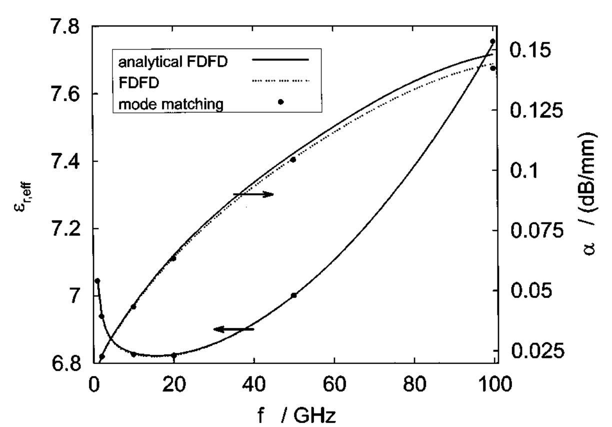

Fig. 6. Slot-line-mode effective permittivity $\varepsilon_{r,\,\mathrm{eff}}$ and attenuation α against frequency (data as in Fig. 3 with electric wall in the center); comparison of the new hybrid method (analytical FDFD) with the conventional FDFD method and mode-matching data [8].

The propagation behavior of the slot-line mode—with an electric wall introduced at $x = a/2$—is plotted in Figs. 6 and 7. As can be seen, effective permittivity exhibits an increase with frequency, which is considerably larger than that of the coplanar mode (see Fig. 4). This indicates dispersion due to non-TEM effects, which also appears in the impedance behavior in Fig. 7.

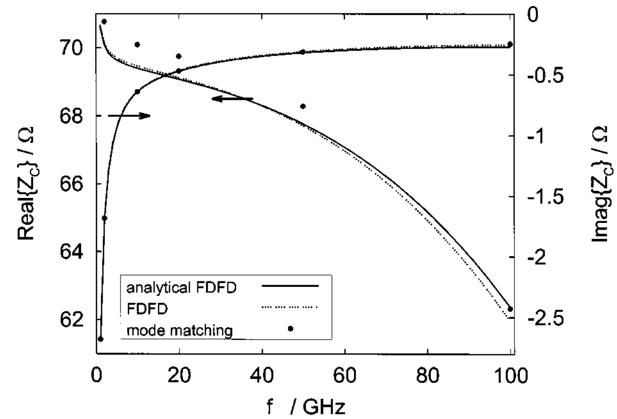

Fig. 7. Slot-line-mode complex characteristic impedance Z_c against frequency (voltage–current definition, other data as in Fig. 6).

In order to understand this, it is helpful to consider the current distributions in the coplanar and slot-line cases. In the coplanar case, the forward current flows on the center conductor and the backward one divides on the two ground planes with strong concentration on the slot sides. A crude model describes this by a line current in the center and two further line currents of opposite direction and one-half the amplitude on the ground planes near the slot. Thus, the characteristic dimension is approximately one-half the ground-to-ground spacing. For the slot-line type, however, the net current on the center conductor vanishes and one has two line currents of opposite direction on the ground planes. The effective characteristic dimension is approximately the ground-to-ground spacing, which is double the value for the coplanar mode. Therefore, the slot-line type shows more pronounced non-TEM effects for the given frequency range.

Comparing the analytical hybrid method with conventional high-resolution full-wave FD results, one finds errors below 0.2% in $\varepsilon_{r,\,\mathrm{eff}}$ and 5% in α, respectively. In the lower millimeter-wave frequency range ($f < 50$ GHz for the CPW mode and $f < 30$ GHz for the slot-line mode), the error in α is below 2%. The deviations in α can be further reduced by taking into account the edge behavior of the transverse magnetic field *outside* the conductor. The relative error in impedance (defined as $|\Delta Z_c/Z_c|$) remains below 1%. The differences between the conventional FD and mode-matching results are less than 0.1% in $\varepsilon_{r,\,\mathrm{eff}}$, 1.3% in α, and 1.2% in Z_c. Altogether, these deviations are fully satisfactory for MMIC design.

Regarding the numerical efforts, the incorporation of correction factors reduces the number of unknowns to approximately 30% and CPU time by a factor of about eight. This is impressive and only slightly offset by the preprocessing efforts in calculating the correction factors according to (5), (6), and (9). Moreover, this procedure can be automated so that the user does not need to deal with the hybrid procedure, but can simply handle the structure as in the lossless case.

In order to establish a reliable basis for verification, further changes in the CPW geometry were considered varying slot-width s and conductor thickness t for a constant ground-to-ground spacing of 50 μm. The results show similar agreement with conventional FDFD and mode-matching results, as found for the data presented in Figs. 4–7.

IV. CONCLUSIONS

Introducing into the FD formulation *a priori* knowledge about the field behavior inside metallic conductors leads to considerable savings in computational cost. This is because skin depth does not determine smallest cell size any more and, therefore, the same discretization, as in the lossless case (ideal conductors), can be applied. For transmission-line analysis of typical MMIC coplanar structures, the number of unknowns is reduced to approximately 30% and CPU time to approximately 13%, achieving an relative error of less than 0.2% in the complex propagation constant $\beta - j\alpha$ and below 1% in the complex impedance Z_c. The original contribution of our approach is that the field behavior within the conductors is described by analytical approximations based on the skin-effect behavior and a special 2-D edge term. Thus, preprocessing can be automated, which leads to an efficient and easy-to-handle FD software tool.

REFERENCES

[1] T. Itoh and R. Mittra, "Spectral-domain approach for calculating the dispersion characteristics of microstrip lines," *IEEE Trans. Microwave Theory Tech.*, vol. MTT-21, pp. 496–499, July 1973.

[2] D. B. Shorthouse and C. J. Railton, "The incorporation of static field solutions into the finite difference time domain algorithm," *IEEE Trans. Microwave Theory Tech.*, vol. 40, pp. 986–994, May 1992.

[3] J. Craddock and C. J. Railton, "A new technique for the stable incorporation of static field solutions in the FDTD method for the analysis of thin wires and narrow strips," *IEEE Trans. Trans. Microwave Theory Tech.*, vol. 46, pp. 1091–1096, Aug. 1998.

[4] S. Lindenmeier, P. Russer, and W. Heinrich, "Hybrid dynamic-static finite-difference approach for MMIC design," in *IEEE MTT-S Int. Microwave Symp. Dig.*, vol. 1, 1996, pp. 197–200.

[5] N.-H. Huynh and W. Heinrich, "FDTD accuracy improvement by incorporation of 3D edge singularities," in *IEEE MTT-S Int. Microwave Symp. Dig.*, vol. 4, 1999, pp. 1573–1576.

[6] M. Kunze and W. Heinrich, "Modified FD formulation for conductor-loss calculation in MMIC coplanar waveguides," in *Proc. Eur. Microwave Conf.*, vol. 2, 1999, pp. 423–426.

[7] ——, "Efficient FD formulation for lossy waveguide analysis based on quasi-static field characteristics," *IEEE Microwave Guided Wave Lett.*, vol. 9, pp. 499–501, Dec. 1999.

[8] W. Heinrich, "Full-wave analysis of conductor losses on MMIC transmission lines," *IEEE Trans. Microwave Theory Tech.*, vol. 38, pp. 1468–1472, Oct. 1990.

[9] T. Weiland, "On the unique numerical solution of Maxwellian eigenvalue problems in three dimensions," *Particle Accelerators*, vol. 17, pp. 227–242, 1985.

[10] J. Geisel, K. H. Muth, and W. Heinrich, "The behavior of the electromagnetic field at edges of media with finite conductivity," *IEEE Trans. Microwave Theory Tech.*, vol. 40, pp. 158–161, Jan. 1992.

[11] K. Beilenhoff and W. Heinrich, "Treatment of field singularities in the finite-difference approximation," in *IEEE MTT-S Int. Microwave Symp. Dig.*, vol. 2, 1993, pp. 979–982.

[12] G. I. Makarov and A. V. Osipov, "Structure of Meixner's series," *Radiophys. Quantum Electron.*, vol. 29, pp. 544–549, 714–720, June 1986. Translated from *Izvestiya Vysshikh Uchebnykh Zavedenii, Radiofizika*.

[13] A. Lauer and I. Wolff, "A conducting sheet model for efficient wide band FDTD analysis of planar waveguides and circuits," in *IEEE MTT-S Int. Microwave Symp. Dig.*, vol. 4, 1999, pp. 1589–1592.

Marco Kunze (S'96) was born in Bremen, Germany, in 1969. He received the Dipl.-Ing. degree from the Technical University Braunschweig, Braunschweig, Germany in 1995, and is currently working toward the Dr.-Ing. degree at the Ferdinand-Braun-Institut für Höchstfrequenztechnik, Berlin, Germany.

From November 1995 to July 1997, he was with the Laboratoire Antennes and Reseaux, University Rennes 1, Rennes, France. Since August 1997, he has been with the Ferdinand-Braun-Institut für Höchstfrequenztechnik, where he is involved in the field of FD electromagnetic simulation.

Wolfgang Heinrich (M'84–SM'95) was born in Frankfurt/Main, Germany, in 1958. He received the Dipl.-Ing., Dr.-Ing., and Habilitation degrees from the Technical University of Darmstadt, Darmstadt, Germany, in 1982, 1987, and 1992, respectively.

In 1983, he joined the staff of the Institute für Hochfrequenztechnik, University of Darmstadt, where he was involved with field-theoretical analysis and simulation of planar transmission lines. Since April 1993, he has been with the Ferdinand-Braun-Institut für Hochfrequenztechnik (FBH), Berlin, Germany, where he is currently Head of the Microwave Department. His current research activities focus on electromagnetic simulation, MMIC design for both GaAs and SiGe with emphasis on the coplanar concept, and flip-chip packaging.